Article:
Norris, D.J., Myronov, M., Leadley, D.R. et al. (1 more author) (2017) Comparison of cross-sectional transmission electron microscope studies of thin germanium epilayers grown on differently oriented silicon wafers. Journal of Microscopy, 268 (3). pp. 288-297. ISSN 0022-2720

https://doi.org/10.1111/jmi.12654

Comparison of Cross-sectional Transmission Electron Microscope Studies of Thin Germanium Epilayers Grown on Differently Oriented Silicon Wafers

D.J. Norris[a], M. Myronov[b], D.R. Leadley[b] and T. Walther[a*]

[a] Kroto Centre for High-Resolution Imaging and Analysis, Department of Electronic and Electrical Engineering, University of Sheffield, Mappin Street, Sheffield, S1 3JD, UK.

[b] Department of Physics, University of Warwick, Gibbet Hill Road, Coventry, CV4 7AL, UK.

* corresponding author: t.walther@sheffield.ac.uk

Keywords: germanium-on-silicon (Ge/Si), islanding, transmission electron microscopy

Abstract

We compare transmission electron microscopical analyses of the onset of islanding in the germanium-on-silicon (Ge/Si) system for three different Si substrate orientations: (001), (1$\bar{1}$0) and (1$\bar{1}$1)Si. The Ge was deposited by reduced pressure chemical vapour deposition and forms islands on the surface of all Si wafers; however, the morphology (aspect ratio) of the deposited islands is different for each type of wafer. Moreover, the mechanism for strain relaxation is different for each type of wafer owing to the different orientation of the (111) slip planes with the growth surface. Ge grown on (001)Si is initially pseudomorphically strained, yielding small, almost symmetrical islands of high aspect ratio (clusters or domes) on top interdiffused SiGe pedestals, without any evidence of plastic relaxation by dislocations, which would nucleate later-on when the islands might have coalesced and then the Matthews-Blakeslee limit is reached. For (1$\bar{1}$0)Si, islands are flatter and more asymmetric, and this is correlated with plastic relaxation of some islands by dislocations. In the case of growth on (1$\bar{1}$1)Si wafers, there is evidence of immediate strain relaxation taking

place by numerous dislocations and also twinning. In the case of untwined film/substrate interfaces, Burgers circuits drawn around certain (amorphous-like) regions show a non-closure with an edge-type a/4[$\bar{1}$12] Burgers vector component visible in projection along [110]. Micro-twins of multiples of half unit cells in thickness have been observed which occur at the growth interface between the Si(1$\bar{1}$1) buffer layer and the overlying Ge material. Models of the growth mechanisms to explain the interfacial configurations of each type of wafer are suggested.

1. Introduction

There is considerable interest in growing thin, epitaxially strained layers (epilayers) of pure Ge (or an alloy of SiGe) onto either buffered Si wafers (Yeo et al. 2005) or onto prepared SiGe virtual substrates (Myronov et al. 2007; Myronov et al. 2014) for research on various quantum phenomena in electronics (Foronda et al. 2015) and spintronics (Morrison and Myronov 2016). The latter virtual substrates are usually comprised of a thick (a few μm) relaxed layer of SiGe grown in a compositionally stepped (Baribeau et al. 1988) or compositionally graded (Fitzgerald et al. 1991; Shah et al. 2010) manner onto a Si wafer on top of which the compressively strained Ge quantum well (QW) epilayer is deposited. The principal gain over Si technology, in terms of final device performance, is the significantly enhanced hole mobility in p-channel Ge QW metal-oxide semiconductor field effect transistor (MOSFET) device structures. Also, Ge nano-pillars may be suitable for photonic applications if their nucleation can be controlled precisely (Pezzoli et al. 2014).

Growth of SiGe on (001)Si commences with the formation on an initially flat wetting layer and then the formation of small islands (Hansson et al. 1992) on the surface of this wetting layer (Stranski-Krastanow growth transition), which has been observed to be related to both lateral and vertical variations of the local chemical composition (Walther, Humphreys and Cullis 1997). Low energy electron microscopy (LEEM) in ultra-high vacuum conditions has been used to study the initial nucleation of small Ge islands on Si(001), showing mesa growth for 2-3 monolayers by step flow (Hannon et al. 2004).

Further work was directed to analysing the morphology of Ge or SiGe islands as they grow and coarsen (Ross, Tersoff and Tromp 1998; Ross, Tromp and Reuter 1999, Tromp and Ross 2000). In particular, in these studies the morphology of quite large island sizes has been

examined by in-situ Transmission Electron Microscope (TEM) with built-in chemical vapour deposition capabilities. Islands were shown to nucleate on the surface in the form of clusters and then developed into pyramidal structures called 'hut-clusters' with rectangular base and {105} facets; with further growth, large-angle facets appeared on the islands and these became dome-like in shape with octagonal base and several types of side facets. It should be emphasised that these islands were much larger than most of the islands investigated here (ours are typically 6-7nm high), because coverage by very small amounts of Ge would have been difficult to study experimentally in plan-view geometry.

More recently, further theoretical enhancement in device performance has been linked to growth of p-channel MOSFET structures on virtual substrates which have been grown on differently oriented wafers; namely (101)Si and (111)Si (Haensch et al. 2006; Makap et al. 2007; Kuzum et al. 2009). However, there are aspects of the microstructure of virtual substrates of this type grown on differently oriented wafers, which are not yet fully understood.

Whilst growth of SiGe virtual substrates on (001)Si wafers produces an adequate surface for growth of a compressively strained SiGe layer, there are inherent difficulties observed in forming similar layer quality on (101) and (111)Si wafers. In the case of growth on (101) surfaces (Hull et al. 1991; Kvam and Hull 1993; Ferrandis and Vescan 2002) there are only two inclined {111} planes which are oriented at ~30° to the substrate normal, and a further two {111} planes which are at 90° to the surface normal. Dislocations that may nucleate along these vertical 90° {111} planes would not be able to glide from the surface through the strained layer down to the interface because of a lack of resolved shear stress (zero Schmid factor) and they could also therefore not be removed from the system, however, as they would have no edge component of their Burgers vector they could not contribute to misfit strain relief anyway. Moreover, a different microstructure appears in this system where stacking faults are generated along inclined {111} planes which are bounded by Shockley partials, and for growth on (111)Si these have been observed to slip into the interfacial (111) plane in surfactant-mediated Ge layers (Horn- von Hoegen et al. 1991; LeGoues et al. 1991; LeGoues et al. 1996). Work has also been done by in-situ growth on plan-view TEM samples (LeGoues et al. 1996) to understand the evolution of Ge islands with steps being an important factor in the formation of the first Ge islands.

There is considerable work directed to the fabrication of virtual substrates of material grown on differently oriented Si wafers (Lee, Antoniadis and Fitzgerald 2006; Hartmann et al. 2008; Arimoto et al. 2009a and 2009b). A predominant feature of SiGe layers grown on (101) surfaces is the occurrence of microtwins that have a deleterious effect on final surface morphology which can be significantly roughened. A comparison has been made of optical interferometry on (100), (101) and (111) of $Si_{1-x}Ge_x$ (x~0.2, Destefanis et al. 2009). This study showed that there is a four-fold symmetric arrangement in the case of (100) surfaces which indeed appears to be consistent with the cross-hatched configuration generated in this system. The (101) surface has a two-fold symmetry which appears to reflect the occurrence of misfit relief in only the two inclined '30°' {111} slip planes. Then, in the case of (111) surfaces, there appears to be significant disorder with misfit relief occurring in the three-fold inclined slip planes. This latter structure appears to have a significantly roughened surface. The temperature dependence of microstructure formation has also been studied, showing a large twinned lamellae structure (Arimoto et al 2008).

In this work, we present a study of the microstructure, via cross-sectional transmission electron microscopy (TEM), of very thin layers of nominally pure Ge grown on a range of differently oriented wafers, with the aim to elucidate early strain relaxation via islanding and plastic deformation.

2. Experimental Details

The Ge epilayers investigated in this study were grown by reduced pressure chemical vapour deposition (RP-CVD) using an ASM Epsilon 2000 reactor on (001), $(1\bar{1}0)$ and $(1\bar{1}1)$ orientated p-type Si substrates. We choose these Miller index notations in the following to denote that all interfaces can be imaged edge-on in the common [110] orientation. The Si substrates were cleaned using a high temperature in-situ H bake immediately prior to epitaxial growth to remove any native oxide. The Ge layers were all grown at 400°C using standard germane (GeH_4) precursor gas at a partial pressure of around 10mTorr (1.3Pa). The growth time for the results on the $(1\bar{1}0)$ and $(1\bar{1}1)$ oriented surfaces shown here was longer (15 minutes) than that used for the growth on the (001) surface (6:36 minutes) due to the longer stagnation times and hence lower growth rates on these surfaces, but all other growth parameters including chamber pressure, H_2 carrier gas flow and wafer rotation speed were

kept constant. The steady-state average growth rate used for the growth of thick Ge layers is around 0.3nm/s; however, this is significantly reduced, by more than one order of magnitude, for growth of the present thin layers because during initial growth there is only a gradual rise in growth rate before eventually the steady state is reached. Since the growth rate of thin SiGe layers in CVD can be markedly different to that of thicker layers (Walther et al. 1997; Walther and Humphreys 1999), due to gas dwell times temperature and desorption of H from the Si(Ge) surface, the actual growth rate of the Ge layer in our case was estimated through TEM measurements. As can be seen from the electron microscopy size measurements summarised in Table 1, these growth conditions yielded comparable average island heights of 6-7nm for all three wafer orientations.

Cross-sectional TEM specimens were fabricated from these wafers in the usual manner by sawing, gluing, grinding and polishing 3mm discs of material followed by argon ion thinning to electron transparency. The wafer was sawn in such a way that the final TEM samples were always viewed along the [110] direction, as determined from the cleaved edges of the wafer. The specimens were then examined using both a JEOL 2010F field-emission gun (FEG-) TEM (197kV) and a JEOL Z3100 R005 (300kV) aberration corrected cold-FEG scanning (S)TEM, both equipped with Gatan Imaging Filters (GIFs) with built-in charge coupled device (CCD) cameras for TEM (a Gatan 1k×1k Multiscan 794 CCD in the JEOL 2010F and a Gatan 2k×2k Ultrascan 1000 CCD in the JEOL R005) as well as bright-field (BF) and annular dark-field (ADF) STEM detectors.

3. Results of Growth of pure Ge on (001), ($1\bar{1}0$) and ($1\bar{1}1$) Si Wafers

3.1 Ge epitaxy upon (001)Si

Cross-sectional high-resolution TEM images of a typical layer of pure Ge grown on (001)Si are shown in figure 1. The Ge layer is not uniformly flat but has instead developed into small islands on the wafer surface. Examples of differently shaped islands are shown in figures 1(a-c). Some islands appear ‘dome-shaped’ with quite steep sloping edges, as in figure 1(a). In figure 1(b), the island is slightly larger than that shown in figure 1(a) and also the edges of the island appear facetted in a plane parallel to one of the two inclined (111)

planes, suggesting that this is a particularly low energy configuration. This also shows that the distinction between small, well facetted hut clusters and larger domes often found in the literature (e.g. Costantini et al. 2005) is somewhat arbitrary, the transition being gradual. In figure 1(c), the island is only ~3nm high, has the form of a spherical calotte and has not yet evolved into a facetted structure. Islands observed here in figure 1 (and also figures 9-11 for $\{1\bar{1}1\}$ orientation) are only 3-6nm high and so significantly smaller than typical SiGe alloy islands observed previously. Presumably, this is because we use a very low growth temperature, and we terminate growth at a point just after the Stranski-Krastanow (SK) transition has occurred. Much work has been done to analyse the morphology of facetted pure Ge islands on (001)Si via in-situ molecular beam epitaxy (MBE)-TEM; and these have identified vital aspects of the size-distribution and the coarsening of the islands into pyramids, huts and domes (Ross, Tersoff and Tromp 1988; Ross, Tromp and Reuter 1999). However, such plan-view TEM experiments proceeded with the observation of relatively large islands, indeed substantially larger than the typical island sizes we have observed in our cross-sectional TEM, presumably due to the weak diffraction contrast evident for the smaller islands. It is therefore difficult to compare these observations directly. Instead, we can assume that were we to grow for longer, our observations would then become consistent with those observed elsewhere.

There is also an indication from bright-field imaging in TEM or STEM mode that the crust surrounding the island appears darker than the material within the body of the island. This dark band on the surface of the wafer to the left and right of the islands visible under bright-field conditions is consistent with both strain and the presence of a Ge-rich wetting layer, the thickness of which is ~3-5 (004) monolayers, i.e. about one unit cell, in all images in figure 1, in agreement with previous observations for CVD grown SiGe (Walther, Humphreys and Cullis 1997) and Ge (Norris et al. 2014).

A High-Angle Annular Dark-Field (HAADF) image of Ge islands on (001)Si is shown in figure 2. Here we see the bright Ge islands on the darker Si wafer material. The islands appear like domes on the surface of the Si wafer, and their centres appear brighter than the island edges because of a possible increase of both the Ge content and the projected thickness here. An interesting feature of this image is that we cannot see the wetting layer clearly. Instead, there appears to be a dark band at the base of the island separating the island from the underlying Si wafer. It is not clear what this dark layer constitutes but a likely

explanation is that the $Si(Ge)O_2$ surface layer formed on the free surface is visible before and/or behind the island as the sample thickness here is much larger than the island extension and we have to take into account that TEM always presents a projection of the specimen structure along the electron beam direction. Only if the specimen thickness does not vary by too much locally, and generally stays below ~100nm, will SiGe always appear brighter in HAADF than pure silicon for any germanium content (Walther and Humphreys 1997), as in figures 3 and 6. Also, the depth of field in HAADF STEM is rather small, and if the image is focused on the island then the wetting layer that extends further along the electron beam direction will appear blurred.

Further studies have been performed on the JEOL Z3100 R005 aberration corrected STEM (see figure 3) and Annular Dark Field images in thinner regions do not appear to show this effect. Instead, the Ge island is grown epitaxially coherent on the Si buffer and seems to stand proud of the surrounding Si crystal on a kind of pedestal ~1nm high. At the same time the Ge-rich wetting layer is of roughly the same width as before but only faintly visible, which can be explained by substantial diffusion of the surrounding Si (and Ge) under and into the lower section of the (Si)Ge island during growth, in agreement with observations of trenches found around Ge islands deposited by molecular beam epitaxy at different temperatures which predicted the onset of interdiffusion to lie in the range of 350-400°C (Smith et al. 2003). While it is not possible to unambiguously index facets from a single projection only, using the standard candidates confirmed from atomic force and scanning tunnelling microscopy measurements of islands (Costantini et al. 2005) the long and flat terraces on the top of the island in figure 3 that are inclined ~25° with respect to (001) and 64° with respect to $(\bar{1}10)$ are likely of {113} type, as predicted by Eaglesham et al. (1993) while the shorter side segments run under ~78° to (001) and therefore may be of $\{0\bar{5}1\}$ type, similar to those of 'hut clusters'. These steeper side facets found in this ~7 nm high island probably constitute the transition from small pyramidal islands as in figure 1 to higher dome-like islands as in figure 2.

We did not find any dislocations, in particular none of the 60° misfit dislocations that have been predicted by Hammar et al. (1996) to relax all Ge islands grown above ~600°C and none of the 90° dislocations observed for Ge deposited by MBE at very low temperatures (Eaglesham and Cerullo 1991), however, our effective Ge coverage has probably been below

the critical thickness for nucleation of these, which was estimated as ~2nm (Fujimoto and Oshiyama 2013).

3.2 Ge epitaxy upon (1$\bar{1}$0)Si

During TEM analysis of samples grown for identical durations on the differently oriented wafers, it was found that, although Ge-rich islands were observed on (001)Si, there did not appear to be any growth of Ge onto the (1$\bar{1}$0)Si or (1$\bar{1}$1)Si wafers in the first minutes. This may be due to differences in adsorption and desorption rates for the growth rates on the different types of wafers (Hartmann et al. 2006). Consequently, two further samples (one on (1$\bar{1}$0)Si and one on (1$\bar{1}$1)Si) were grown with increased deposition time of the original samples as stated above. Atomic Force Microscopy revealed that, this time, Ge material was indeed deposited.

For growth of Ge upon (1$\bar{1}$0)Si, islands are again observed; however, they appear more elongated, as shown in figure 4. The island is ~60nm in wide at its base and ~8nm high, does not reveal any clear faceting and does not contain any dislocation despite its relatively large volume We observe in the (1$\bar{1}$0)Si wafer, however, that relaxation of misfit strain energy can occur via the nucleation of Shockley partial dislocations (Kvam and Hull 1993) from the surface of the island and glide down to the island/wafer interface, as shown in figure 5.

Further analysis has been done using Annular Dark-Field (ADF) imaging and a typical region is shown in figure 6. Here we see the elongated islands clearly and again the wetting layer as a bright band of around 1nm thickness on the surface of the wafer in between the islands. All islands in figures 3-6 are ~7nm high, suggesting a growth rate under 0.47nm/minute. Measurements of growth rates from thick relaxed Ge layers on (101)Si yielded an average steady-state growth rate of ~0.1nm/s at 400°C (Nguyen et al. 2012), demonstrating initial growth is slowed down significantly.

3.3 Ge epitaxy upon (1$\bar{1}$1)Si

Perhaps the most interesting of these samples is the Ge deposited on (1$\bar{1}$1)Si. As an overview of the morphology, a low magnification Annular Dark-Field image is provided in figure 7.

Here, the bright Ge layer is clear, and it appears that the coverage of the underlying wafer is greater than in the previous wafer discussed above. There are regions where the islands are narrow, but there are regions also where large terraces of deposited material can be found, yielding one undulating thin film. This would suggest that the islands are initially small and then subsequently merge with further growth. However, this is the closest we have got to obtaining an almost continuous layer of Ge on the surface of the wafer instead of small dome-like islands as observed in the (001)Si wafer case. The maximum thickness of the Ge layer on $(1\bar{1}1)$Si of 6 nm corresponds to an upper limit of the growth rate of 0.4nm/min, which is lower than the (001) value by a factor of 2. It is also clear that the surface of this 'pseudo'-continuous layer is rough, with an amplitude of roughness of ~4nm. Again, growth of thick relaxed Ge layers on $(1\bar{1}1)$Si yielded an average growth rate of 0.05nm/s at 400°C (Nguyen et al. 2012) which is slow but still significantly higher than what we observe at the onset of islanding.

If the thinnest region of the TEM specimen is now focused upon, where the material is suitable for high resolution phase contrast imaging, we observe discrete islands such as the one shown in figure 8. This image is obtained using the JEOL 2010F analytical TEM and shows clearly the atomic columns close to the island/wafer interface. There appear to be small regions on this boundary which are amorphous-like in appearance. If a Burgers circuit is drawn around these nano-scale regions, as indicated in figure 8(b), we find that the centres of these regions contain dislocation cores. They appear similar to Lomer dislocations imaged by Vanhellemont et al. (1988) but the crystal orientation here is with $[1\bar{1}1]$ instead of [001] pointing upwards, and the attributed Burgers vector in our case is $\underline{\mathbf{b}}_e$=a/4 $[\bar{1}12]$. This is not a recognised Burgers vector of any perfect or partial dislocation in face-centred crystals, however, the Burgers vector of our dislocation may also have a component along the electron beam direction, which would be invisible in this projection. Assuming a screw component of $\underline{\mathbf{b}}_s$=a/4 [110] would mean that these dislocations could be of a mixed type with standard (i.e. the most common) Burgers vector $\mathbf{b}$=a/2[011]=$\underline{\mathbf{b}}_e$+$\underline{\mathbf{b}}_s$ of which we see only the edge component in the [110] zone axis. The amorphous-like appearance of the dislocation cores is probably due to the (invisible) screw component $\underline{\mathbf{b}}_s$ distorting the crystal along the electron beam direction, in particular where it penetrates the free surface and leads to strain relaxation, twisting the crystal around its core (Eshelby 1953).

One other important factor when trying to compare growth in these three systems is to ensure that the surface normal of the substrate is parallel with the intended low-index plane. If these two parameters separate then a substrate offcut is introduced with a substantial increase in the surface step density. In the case of growth on the (001) and ($1\bar{1}0$) samples, as above, no offcut was observed. This was not the case with the ($1\bar{1}1$)Si wafer; here, if we examine figure 9, we see a substantial offcut of ~2° between the surface normal and ($1\bar{1}1$)Si. The actual offcut may be even higher than this if the perpendicular component (the vector component parallel along the beam direction) also deviates substantially from the zone axis. This may influence the morphology of the finally grown layer making the island non-symmetrical in terms of the slope of the edges of the islands as observed in figure 9. Unfortunately, there has not been any opportunity for X-ray diffraction of a larger wafer piece, which may be useful to perform in the future.

One interesting feature of the present ($1\bar{1}1$)Si grown wafer is the occurrence of twinning. Since the basal (habit) plane is {111} type, there is a possibility that the (001) direction of deposited material can be oriented in one of two ways. Either the (001) direction can follow the (001) direction of the substrate wafer. Or, alternatively, a twinned configuration can be established whereby the (001) of the deposited material is mirrored about the interface plane. An example of this can be seen in figure 10 (Norris et al. 2011). Here, we see a grain (indexed B) which is a mirror twin of the underlying substrate and bounded by partial dislocations. The surrounding Ge islands (grains A and C) show the same amorphous-like mixed-type dislocation core structures as discussed before, of which only the edge components are visible along [110] zone axis. This would indicate that twinning (essentially a stacking fault accompanied by partial dislocations) may be regarded as an alternative to the introduction of complete misfit dislocations; however, the situation is more complicated than that. If the microscope point resolution is sufficient to resolve individual atomic columns of the diamond structure along the <110> zone axis (so-called dumb-bells), i.e. better that 0.13 nm, we can determine at the atomic level the orientation of these dumb-bells, which are aligned along the (001) orientation of the local crystal lattice.

From the image shown in figure 11, taken using the JEOL Z3100 R005, it can be clearly seen that there is a switching of orientation of the Ge dumb-bells at various regions of the interface (these areas are marked in transparent yellow colour in figure 11). Upon further growth of the island the orientation of the (004)Ge lattice planes reverts back to the correct

alignment where they are parallel to those dumb-bells of the underlying Si wafer. These microtwins observed at the boundary between the deposited island and the underlying wafer are very narrow and found to be always exactly 2 monolayers (= ½ unit cell), 4 monolayers (=1 unit cell) or 6 monolayers (=1 ½ unit cell) in thickness. Their origin is still unclear, although it is likely due to the offcut producing numerous steps on the growth surface and the energy of formation of the twinned orientation being very low so growth on a $(1\bar{1}1)$Si wafer has the option of adopting a non-mirror or a mirrored orientation.

4. Discussion

It is evident that the initial growth of pure Ge upon a Si wafer has implications in terms of final layer morphology. Indeed, the growth mechanism for a misfit system is governed by the difference in lattice parameters of the deposit and the substrate. In the case of Si and Ge, the lattice parameters a, at room temperature, are 0.5431nm and 0.56575nm respectively, giving a misfit of ~4.2%.

There are a number of growth modes that can occur in lattice matched and lattice mismatched systems. For lattice matched systems growth tends to adopt the Frank-van de Merwe (layer-by-layer) mode of growth. For lattice mismatched systems, growth can adopt the Volmer-Weber (islanding) mode or the Stranski-Krastanow (SK, layer-by-layer followed by islanding) mode. In the present system islands appear to form on a very thin 'wetting' layer, which shows the present system follows the Stranski-Krastanow growth as expected. Other compressively strained systems, such as the InGaAs/GaAs system, also display growth according to the SK mode, and the mechanism which governs this behaviour has been explained in terms of segregation/intermixing processes during the initial stages of growth with significant enrichment of In at the surface (Cullis et al. 2002).

Indeed, in the initial stages of growth, the Ge that adheres to the Si surface is initially pseudomorphic. Exchange (intermixing) processes between the upper-most layers of atoms mean that the topmost monolayer can initially become slightly diluted by intermixing with the underlying Si, and it may take a few more monolayers of growth for Ge enrichment to occur, until the surface reaches the concentration of pure Ge. However, there is a certain critical surface concentration below which layer-by-layer growth is maintained, but above which the layer undergoes the SK transition whereupon islands start to nucleate. It may be

that the presence of a very Ge enriched surface monolayer, as observed for SiGe deposition (Walther, Humphreys and Cullis 1997; Walther, Humphreys, and Robbins 1997; Smith et al. 2003; Radtke et al. 2013), affects the adsorption and desorption rates of deposited material such that these rates are similar, and deposition proceeds by finding 'weak' points of low energy, such as step edges or other stress concentrations on the deposit surface, where islands can nucleate.

During the growth of pure Ge, there are only a small number of monolayers of growth before the uppermost (surface) monolayer exceeds the critical concentration and the SK transition is triggered (Norris et al. 2014). However, if the Ge layer is diluted with Si during deposition, then it is possible that the wetting layer can be thicker prior to the onset of islanding (Walther et al. 2013).

The different aspect ratios for growth on the differently oriented wafers suggest that there are differences in the surface tension as well as in the energies of adatoms, dimers, and reconstructed surface steps of material adhering to the wafer surface for different orientations. Surface tension should be stronger for surfaces with more strongly inclined facets, but the scatter of sidewall inclinations in Table 1 is too large to allow us to draw any useful conclusion. In fact, only the values for $(1\bar{1}0)$ are consistently small, while Eaglesham et al. (1993) predicted the surface tension of both {110} and {001} surfaces to be very high.

In the case of growth upon the (001)Si surface, we showed a selection of images of differently shaped islands of a range of sizes. These islands are particularly small and form at a point quite close to the SK transition. However, we should consider the geometry of the specimen in determining the shape of the islands we observe. A Scanning Tunnelling Microscopy (STM) review (Motta 2002) of islanding on (001)Si and (111)Si shows that in the case of Ge grown on (001)Si, the islands formed are initially a truncated pyramidal structure with a square base. These then grow to form domes, and then they can become elongated to form rectangular huts on the (001)Si surface. It appears that these huts have long edges which are parallel to the {100}Si direction. If this is the case then our specimens will be viewed at 45° to these edges, as the electron beam direction is parallel with the <110>Si type direction. This would therefore distort the apparent shape of the island. However, these hut-like features occur quite late on in the growth process and should be much larger than the island features we observe here. The larger of the islands shown here (figure 1b) appears to have facetted edges, and this may reflect the onset of formation of a

truncated pyramid. It was necessary, however, to produce specimens with the island/substrate interface oriented in the <110> orientation, as we have adopted, so that misfit dislocation features observed at this interface could be clearly examined. Moreover, since the islands reported elsewhere are larger than those discussed here, by an order of magnitude, it is difficult to make a detailed comparison.

In the case of growth upon the $(1\bar{1}1)$Si surface, we observed what seems to be an array of dislocations at the island/substrate interface. A Burgers circuit around the amorphous-like regions showed non-closure; however, the closing vector $\mathbf{b}_e=a/4[\bar{1}12]$ does not seem to represent the full Burgers vector but only the edge component of a mixed-type dislocation which is inclined to the beam direction to give a conventional **a**/2[011] vector. So, what is observed in figures 8-10 is a projection of the Burgers vector along the electron beam direction. Such a/2[011] dislocations will be quite efficient at relieving interfacial misfit because both the (relatively large) edge component and the (smaller) screw component of the Burgers vector lie completely in the $(1\bar{1}1)$ interface plane, whereas typical 60º misfit dislocations in the other two systems ((001) and $(1\bar{1}0)$) would be inclined.

For a dislocation with a/2[011] Burgers vector in a $(1\bar{1}1)$ oriented sample there will be sufficient resolved shear stress to make it glide from the wafer surface to the interface on a (111) glide plane. This is reminiscent of dislocations introduced in materials which grow via the Volmer-Weber growth mode where growth proceeds immediately in a 3D islanding mode and relieves misfit strain energy quite efficiently by introducing dislocations at the edges of islands as the island size increases. What is clear is that misfit relief in the $(1\bar{1}1)$Si system proceeds with a way of introducing dislocations with Burgers vector in the $(1\bar{1}1)$ habit plane parallel to the island/wafer interface. In any case, this may have important implications in that it may be difficult to produce pseudomorphically strained layers on such $(1\bar{1}1)$Si wafers.

Microtwins are observable even at moderate lattice resolution, however, measuring the precise number of individual (004) monolayers they consist of necessitates a resolution sufficient to resolve individual (004)Ge 'dumb-bells'. The $(1\bar{1}1)$ surface acts as a mirror plane and allows growth in one of two configurations where (004)Ge is aligned with that of the substrate or grows in a mirror related twin configuration. Both alternatives seem energetically equally favourable and, given stacking faults are always bounded by partial dislocations, are perhaps evidence of a misfit relieving mechanism in this system. Moreover,

it appears that with further growth the required (001)Si//(001)Ge epitaxial relationship is obtained as the microtwins achieve a lateral length of only typically 6-7 nm and so cover only a small fraction of the substrate. These twin structures appear to be buried, confined to the film-substrate interface, and do not have components which extend up to the final free surface.

5. Conclusions

Islanding occurs in all samples and this has been attributed to the SK transition which likely occurs as a result of Ge segregation and intermixing within the uppermost Si monolayers of the wafer, and here an instability arises due to Ge surface enrichment during growth of the initially flat wetting layer.

Growth on (001)Si wafers gives rise to islands with small aspect ratios of 5 ± 1 (base width/height) with sharper sloping edges. The growth on $(1\bar{1}0)$ and (101)Si produces flatter islands with larger aspect ratios of 9 ± 2, at about similar average coverage but with much reduced initial growth rates.

Images have shown that strained pseudomorphic growth occurs on (001) and $(1\bar{1}0)$ surfaces; however, on $(1\bar{1}1)$ surfaces it has been shown through high resolution images that an array of misfit relieving dislocations are present at the island/substrate interface indicating that the islands are not fully strained. This has been explained in terms of the presence of a slip/glide plane parallel to the film substrate interface along which misfit dislocations can be introduced. These dislocations are mixed type and probably have the usual **a**/2<110> Burgers' vector. A novel configuration of microtwins has also been observed at a portion of the Ge/Si$(1\bar{1}1)$ interface where the twins appear to be confined to the interface and don't extend up to the surface.

Acknowledgements

The authors thank the Engineering and Physical Sciences Research Council for financial support of this work under grant number EP/F033893/1 "Renaissance Germanium".

References

Arimoto, K, Watanabe, M., Yamanaka, J., Nakagawa, K., Sawano, K, Shiraki, Y., Usami, N. and Nakajima, K. (2008) Growth temperature dependence of the crystalline morphology of SiGe films grown on Si(110) substrates with compositionally step-graded buffer. Thin Solid Films **517**:1, 235-238.

Arimoto, K, Watanabe, M., Yamanaka, J., Nakagawa, K., Sawano, K, Shiraki, Y., Usami, N. and Nakajima, K. (2009a) Strain relaxation mechanisms in compositionally uniform and step-graded SiGe films grown on Si(110) substrates. Solid-State Electronics **53**:10, 1135-1143.

Arimoto, K, Watanabe, M., Yamanaka, J., Nakagawa, K., Sawano, K, Shiraki, Y., Usami, N. and Nakajima, K. (2009b) Crystalline morphologies of step-graded SiGe layers grown on exact and vicinal Si(110) substrates. J. Cryst. Growth **311**:3, 809-813.

Baribeau, J.M., Jackman, T.E., Houghton, D.C.Maigné, P. and Denhoff. M.W. (1988) Growth and characterization of $Si_{1-x}Ge_x$ and Ge epilayers in (100)Si. J. Appl. Phys. **63**:12, 5738-5746.

Costantini, G., Rastelli, A., Manzano, C., Acosta-Diaz, P., Katsaros, G. Songmuang, R., Schmidt, O.G., v. Känel, H. and Kern, K. (2005) Pyramids and domes in the InAs/GaAs(001) and Ge/Si(001) systems. J. Cryst. Growth **278**:1-4, 38-45.

Cullis, A.G., Norris, D.J., Walther, T., Migliorato, M.A. and Hopkinson M (2002) Stranski-Krastanow transition and epitaxial island growth. Phys. Rev. B **66**:8, 081305R.

Destefanis, V., Hartmann, J.M., Abbadie, A., Papon, A.M. and Billon, T. (2009) Growth and structural properties of SiGe virtual substrates on Si(100), (110) and (111). J. Cryst. Growth **311**:4, 1070-1079.

Eaglesham D.J. and Cerullo, M. (1991) Low-temperature growth of Ge on Si(100). Appl. Phys. Lett. **58**:20, 2276-2278

Eaglesham, D.J., White, A.E., Feldman, L.C., Moriya, N. and Jacobson, D.C. (1993) Equilibrium shape of Si. Phys. Rev. Lett. **70**:11, 1643-1646.

Eshelby, J.D. (1953) Screw dislocations in thin rods. J. Appl. Phys. **24**, 176-179.

Ferrandis, P. and Vescan, L. (2002) Growth and characterization of Ge islands on Si(110). Mater. Sci. & Engn. B **89**:1-3, 171-175.

Fitzgerald E.A., Xie, Y.H., Green, M.L., Brasen, D., Kortan, A.R., Michel, J., Mill, Y.J. and Weir, B.E. (1991) Totally relaxed Ge_xSi_{1-x} layers with low threading dislocation densities grown on Si substrates. Appl. Phys. Lett. **59**:7, 811-813.

Foronda, J., Morrison, C., Halpin, J.E., Rhead, S.D. and Myronov, M. (2014). Weak antilocalization of high mobility holes in a strained Germanium quantum well heterostructure. J. Phys. Cond. Matter **27**:2, 022201.

Fujimoto, Y and Oshiyama, A. (2013) Structural stability and scanning tunnelling microscopy images of strained Ge films in Si(001). Phys. Rev. B **87**:7, 075323.

Haensch, W., Nowak, E.J., Dennard, R.H., Solomon, P.M., Bryant, A., Dokumaci, O.H., Kumar, A., Wang, X., Johnson, J.B. and Fischetti, M.V. (2006) Silicon CMOS devices beyond scaling. IBM J. Res. Dev. **50**:4-5, 339-361.

Hammar, M., LeGoues, F.K., Tersoff, J. , Reuter, M.C. and Tromp, R.M. (1996) In situ ultrahigh vacuum transmission electron microscopy studies of hetero-epitaxial growth I. Si(001)/Ge. Surface Sci. **349**, 129-144.

Hannon, J.B., Copel, M., Stumpf, R., Reuter, M.C. and Tromp, R.M. (2004) Critical role of surface steps in the alloying of Ge on Si(001). Phys. Rev. Lett. **92**:21, 216104.

Hansson, P.O., Albrecht, M., Strunk, H.-P., Bauser, E. And Werner, J.H. (1992) Dimensionality and critical sizes of GeSi on Si(100). Thin Solid Films **216**:2, 199-202.

Hartmann, J.M., Burdin, M., Rolland, G. and Billon, T. (2006) Growth kinetics of Si and SiGe on Si(100), Si(110) and Si(111). J. Cryst. Growth **294**:2, 288-295.

Hartmann, J.M., Papon, A.M. Destefaniz, V. and Billon, T. (2008) Reduced chemical vapor deposition of Ge thick layers on Si(001), Si(011) ad Si(111). J. Cryst. Growth **310**:24, 5287-5296.

Horn- Von Hoegen, M., LeGoues, F.K., Copel, M., Reuter M.C. and Tromp R.M. (1991) Defect self-annihilation in surfactant-mediated epitaxial-growth. Phys. Rev. Lett. **67**:9, 1130-1133.

Hull, R., Bean, J.C., Peticolas, L. and Bahnck, D. (1991) Growth of Ge_xSi_{1-x} alloys on Si(110) surfaces. Appl. Phys. Lett. **59**:8, 964-966.

Kuzum, D., Pethe, A.J., Krishnamohan, T. and Saraswat, K.C. (2009) Ge (100) and (111) n- and p-FETs with high mobility and low-T mobility characterization. IEEE Trans. Electron Devices **56**:4, 648-655.

Kvam, E.P. and Hull, R. (1993) Surface orientation and stacking fault generation in strained epitaxial growth. J. Appl. Phys. **73**:11, 7407-7411.

Lee, M.L., Antoniadis, D.A. and Fitzgerald, E.A. (2006) Challenges in epitaxial growth of SiGe buffers on Si (111), (110) and (112). Thin Solid Films **508**:1-2, 136-139.

LeGoues, F.K., Horn-Von Hoegen, M., Copel, M. And Tromp. R.M. (1991) Strain-relief mechanism in surfactant-grown epitaxial germanium films on Si(111). Phys. Rev. B **44**:23, 12894-12902.

LeGoues, F.K., Hammar, M., Reuter, M.C. and Tromp, R.M. (1996) In situ TEM study of the growth on Si(111). Surf. Sci. **349**:3, 249-266.

Maikap, S., Lee, M.H., Chang, S.T. and Liu, C.W. (2007) Characteristics of strained-germanium p- and n-channel field effect transistors on a Si (111) substrate. Semicond. Sci. Technol. **22**:4, 342-347.

Morrison, C. and Myronov M. (2016). Strained germanium for applications in spintronics. physica status solidi (a) **213**:11, 2809-2819.

Motta, N. (2002) Self-assembling and ordering of Ge/Si(111) quantum dots: scanning microscopy probe studies. J. Phys.: Cond. Matter **14**:35, 8353-8378.

Myronov, M., Sawano, K., Shiraki, Y. Mouri, T. and Itoh, K.M. (2007) Observation of two-dimensional hole gas with mobility and carrier density exceeding those of two-dimensional electron gas at room temperature in the SiGe heterostructures. Appl. Phys. Lett. **91**:8, 082108.

Myronov, M., Morrison, C., Halpin, J., Rhead, S., Casteleiro, C., Foronda J., Shah V.A. and Leadley, D. (2014) An extremely high room mobility of two-dimensional holes in a strained Ge quantum well heterostructure grown by reduced pressure chemical vapor deposition. Japan. J. Appl. Phys **53**:4, 04EH02.

Nguyen, V.H., Dobbie, A., Myronov, M., Norris, D.J., Walther, T. and Leadley, D.R. (2012) Epitaxial growth of relaxed germanium layers by reduced pressure chemical vapour deposition on (110) and (111) silicon substrates. Thin Solid Films **520**:8, 3222-3226.

Norris, D.J., Ross, I.M., Dobbie, A., Myronov, M., Whall, T.E., Parker, E.H.C., Leadley, D.R. and Walther T. (2011) A TEM study of Ge-on-(111)silicon structures for potential use in high performance PMOS device technology. J. Phys.: Conf. Ser. **326**, 012023.

Norris, D.J., Qiu, Y., Dobbie, A., Myronov, M. and Walther, T. (2014) Similarity of Stranski-Krastanow growth of Ge/Si and SiGe/Si. J. Appl. Phys. **115**:1, 012003.

Pezzoli, F., Isa, F., Isella, G., Falub, C.V., Kreiliger, T., Salvalaglio, M., Bergamaschini, R. , Grilli, E., Guzzi, M., von Kaenel, H. and Miglio, L. (2014) Ge crystals on Si show their light. Phys. Rev. Applied **1**:4, 044005.

Radtke, G., Favre, L., Couillard, M., Amiard, G., Berbezier, L. and Botton. G.A. (2013) Atomic-scale Ge diffusion in strained Si revealed by quantitative scanning transmission electron microscopy. Phys. Rev. B **87**:20, 205309.

Ross, F.M., Tersoff, J. and Tromp, R.M. (1998) Coarsening of self-assembled Ge quantum dots on Si(001). Phys. Rev. Lett. **80**:5, 984-987.

Ross, F.M., Tromp, R.M. and Reuter, M.C. (1999) Transition states between pyramids and domes during Ge/Si island growth. Science **286**:5446, 1931-1934.

Shah, V.A., Dobbie, A., Myronov M. and Leadley, D.R. (2010). Reverse graded SiGe/Ge/Si buffers for high-composition virtual substrates. J. Appl. Phys. **107**:6, 064304.

Smith, D.J., Chandrasekhar, D., Chaparro, S.A., Crozier, P.A., Drucker, J., Floyd, M., McCartney, M.R. and Zhang, Y. (2003) Microstructural evolution of Ge/Si(100) nanoscale islands. J. Crystal Growth **259**:3, 232-244.

Tromp , M.C. and Ross, F.M. (2000) Advances in in-situ ultra-high vacuum electron microscopy: growth of SiGe on Si. Annu. Rev. Mater. Sci. **30**,431-449.

Vanhellemont, J., de Boeck, J., Aharoni, H. and Borgs, G. (1988) TEM study of MBE GaAs grown on silicon substrates. Proc. EUREM'88, York, Inst. Phys. Conf. Ser. **93**, 79-80.

Walther, T. and Humphreys, C.J. (1997) Quantification of the composition of silicon germanium / silicon structures by high-angle annular dark field imaging. Proc. EMAG-97, Cambridge, UK. Inst. Phys. Conf. Ser. **153**, 303-306.

Walther, T. and Humphreys, C.J. (1999) A quantitative study of compositional profiles of chemical vapour-deposited strained silicon-germanium / silicon layers by transmission electron microscopy. J. Cryst. Growth **197**:1-2, 113-128

Walther, T., Humphreys, C.J. and Cullis, A.G. (1997) Observation of vertical and lateral Ge segregation in thin undulating SiGe layers on Si by electron energy loss spectroscopy, Appl. Phys. Lett. **71**:6, 809-811.

Walther, T., Humphreys, C.J., Cullis, A.G. and Robbins, D.J (1997) A study of interdiffusion and germanium segregation in low-pressure chemical vapour deposition of SiGe / Si quantum wells. Proc. MSM-10, Oxford, UK. Inst. Phys. Conf. Ser. **157**, 47-54.

Walther, T., Humphreys, C.J. and Robbins, D.J (1997) Diffusion and surface segregation in thin SiGe / Si layers studied by scanning transmission electron microscopy. Defect Diffusion Forum **143**:2, 1135-1140.

Walther, T., Norris, D.J., Qiu, Y., Dobbie, A., Myronov, M. and Leadley, D.R. (2013) The Stranski-Krastanow transition in SiGe epitaxy investigated by scanning transmission electron microscopy. phys. stat. sol. (a) **210**:1 (2013) 187-190.

Yeo, C.C., Cho, B.J., Gao E., See, S.J., Lee, A.H., Yu, C.Y., Liu, C.W. , Tang, L.J. and Lee, T.W (2005) Electron mobility enhancement using ultrathin pure Ge on Si substrate. IEEE Electron Device Lett., **26**:10, 761-763.

figure	wafer orientation	height [nm]	length [nm]	sidewall inclination [°]
1a	(001)	6	24	45-55
1b	“	6	29	44-56
1c	“	3	19	22-25
2	“	(8), 11	29	45-65
3	“	7	19	60-75
		6.8±2.6	**24±5**	
4	$(1\bar{1}\,0)$	8	53	10-35
5	“	7	-	~12
6	“	6, 7	50, 58	20-30
		7.0±0.8	**54±4**	
7	$(1\bar{1}\,1)$	7, 8	116, 92	20-40
8	“	9	28	30-70
9	“	6	42	~40
10	“	5, 3.5, 4	14	70-80
11	“	5	-	-
		6.0±1.9	**58±44**	

Table 1 : List of island dimensions measured from electron micrographs

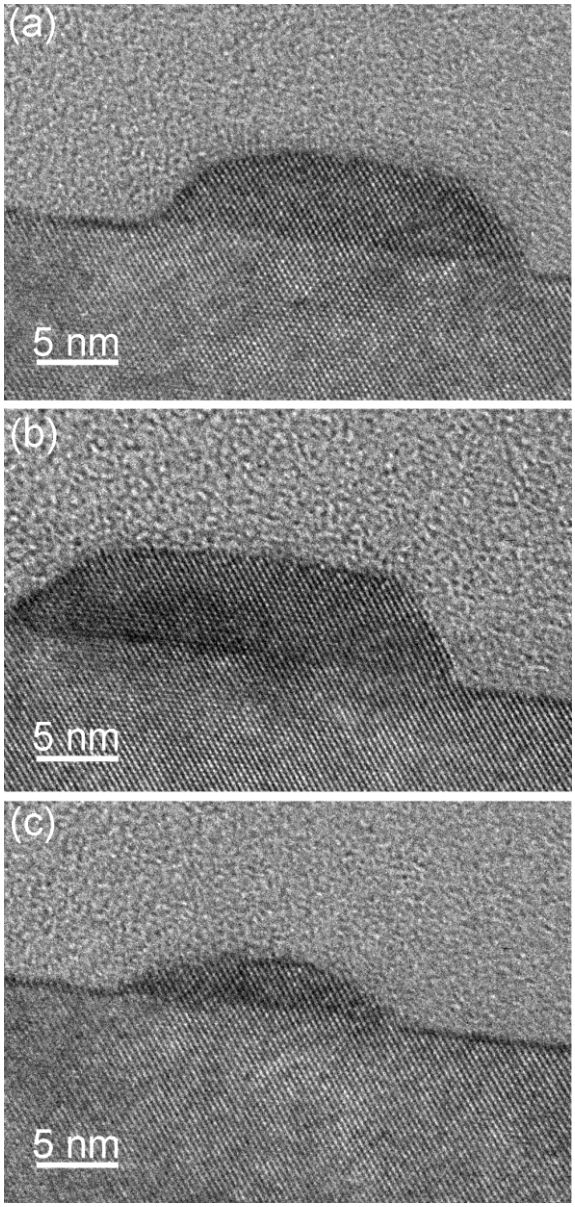

Figure 1. Phase contrast images of (a) dome-shaped island with ~50° sidewall inclination, (b) faceted hut-type cluster and (c) smaller island with 20-25° sidewall inclination of Ge grown on (001)Si.

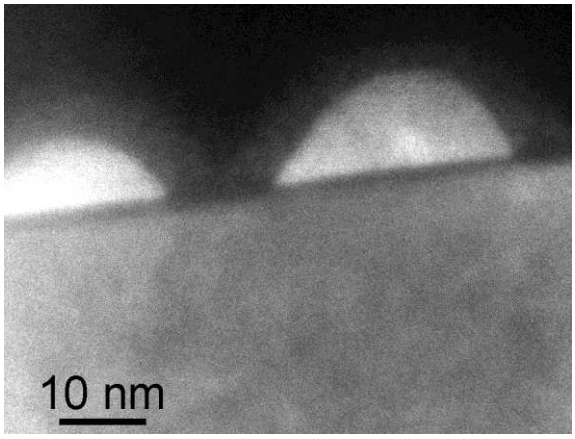

Figure 2. Annular Dark Field image of largest, asymmetric dome-shaped Ge islands on (001)Si.

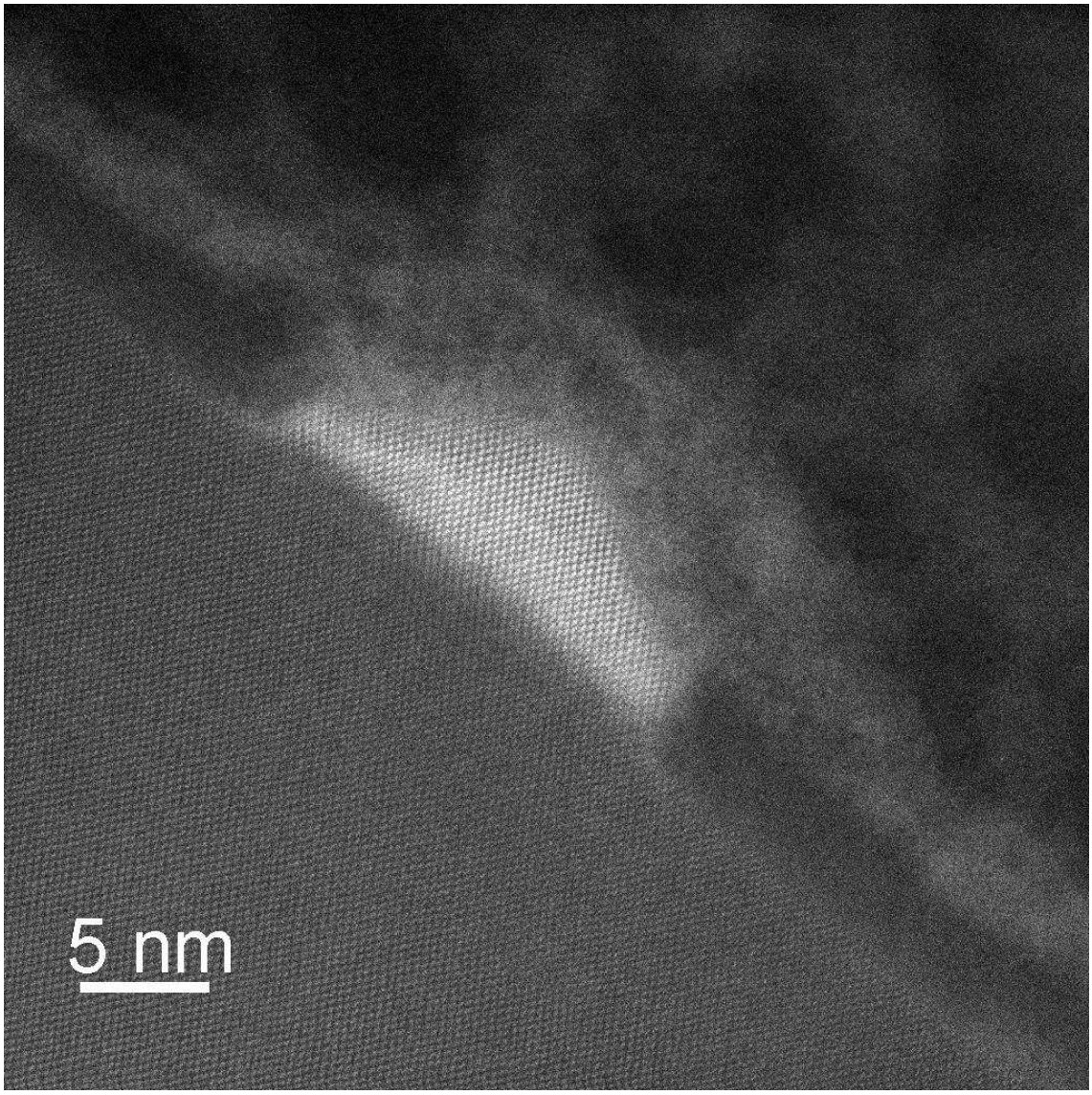

Figure 3. High Resolution Annular Dark Field image of Ge island on (001)Si, showing trench formation around the island which then stands proud on an alloyed SiGe pedestal

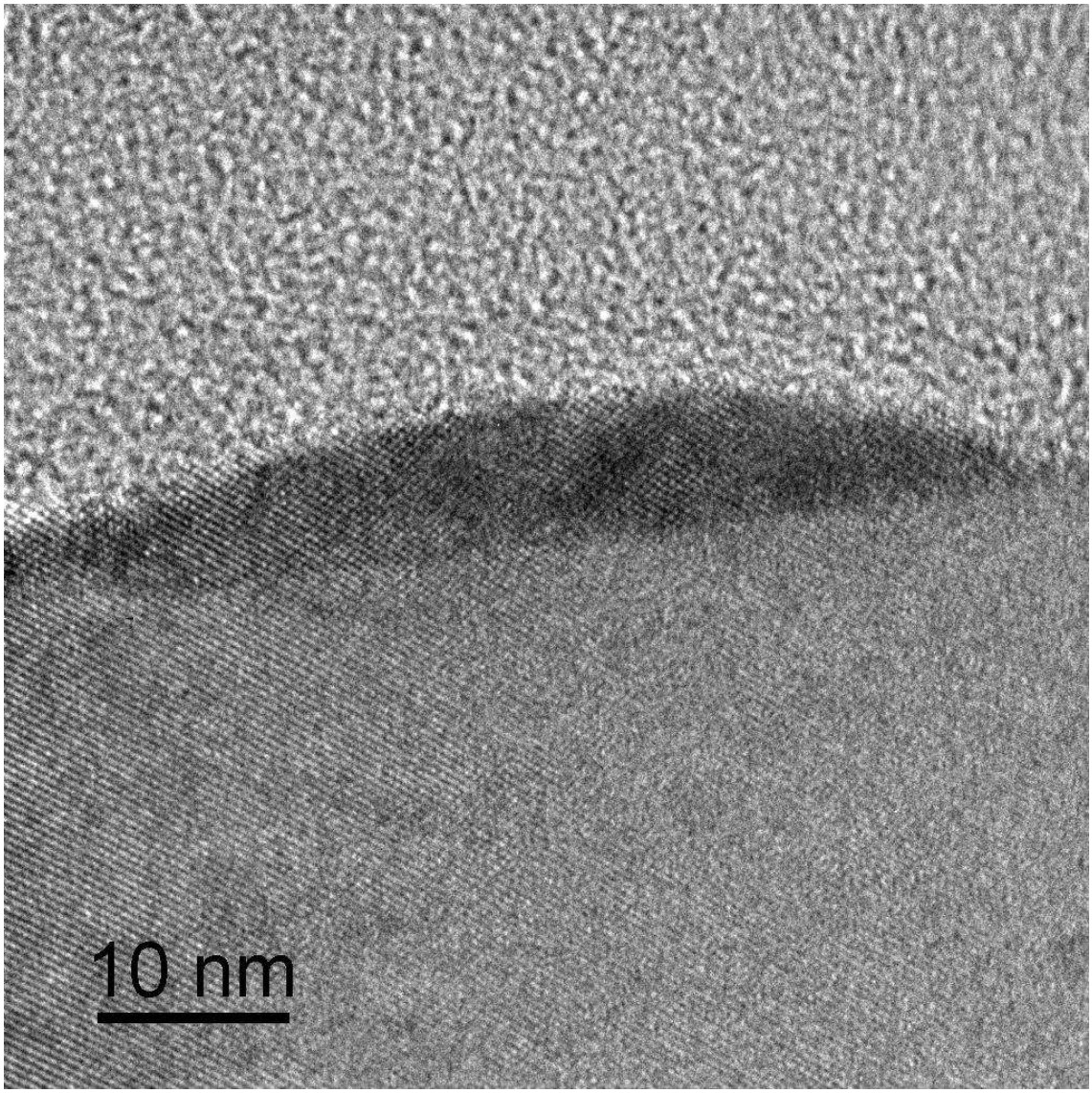

Figure 4. Dilated island with ~20° sidewall inclination on the right observed for Ge grown on (1$\bar{1}$ -0)Si.

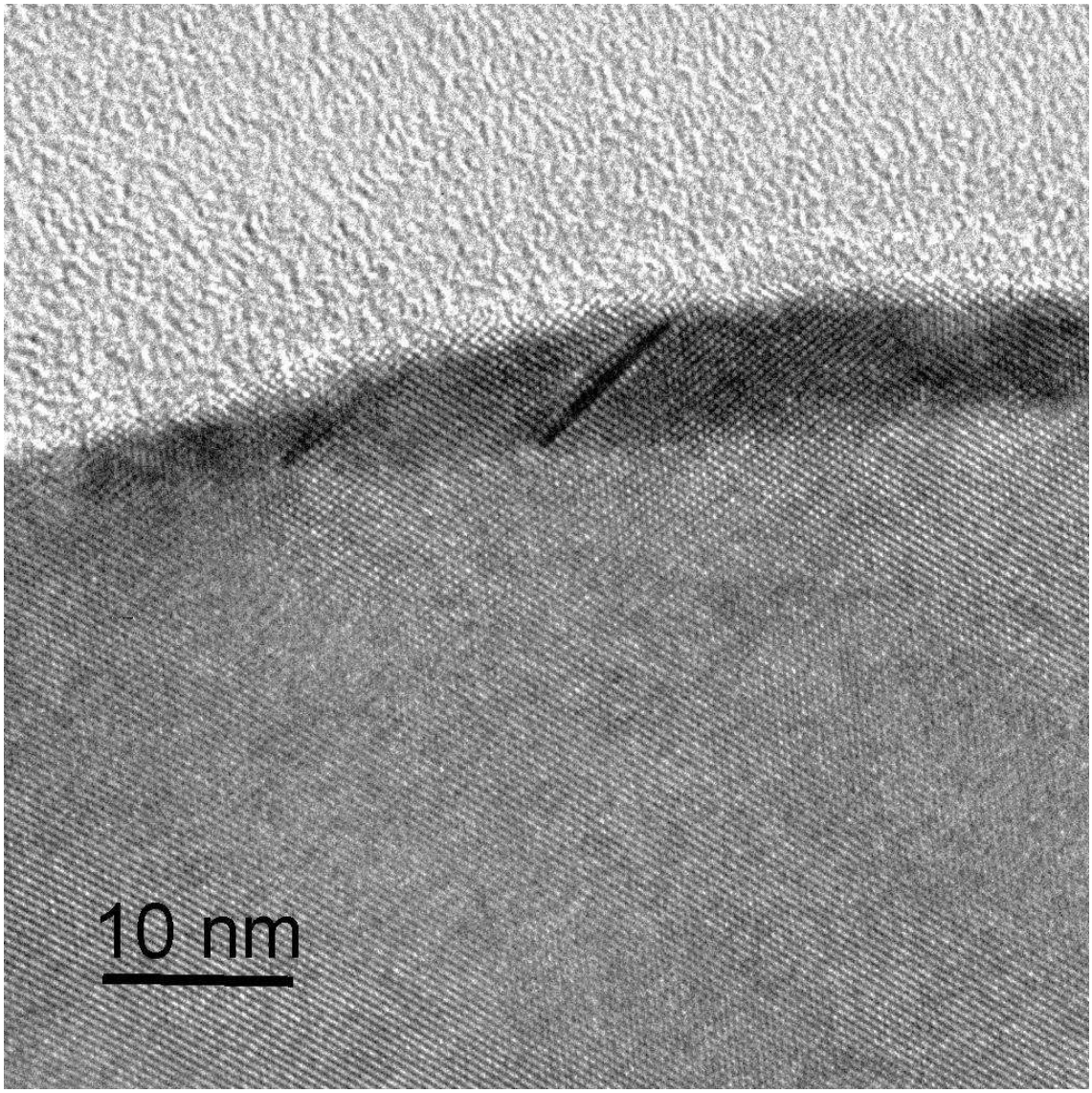

Figure 5. Nucleation of a stacking fault at the surface, ending in a partial dislocation at the interface of Ge grown on (1$\bar{1}$0)Si.

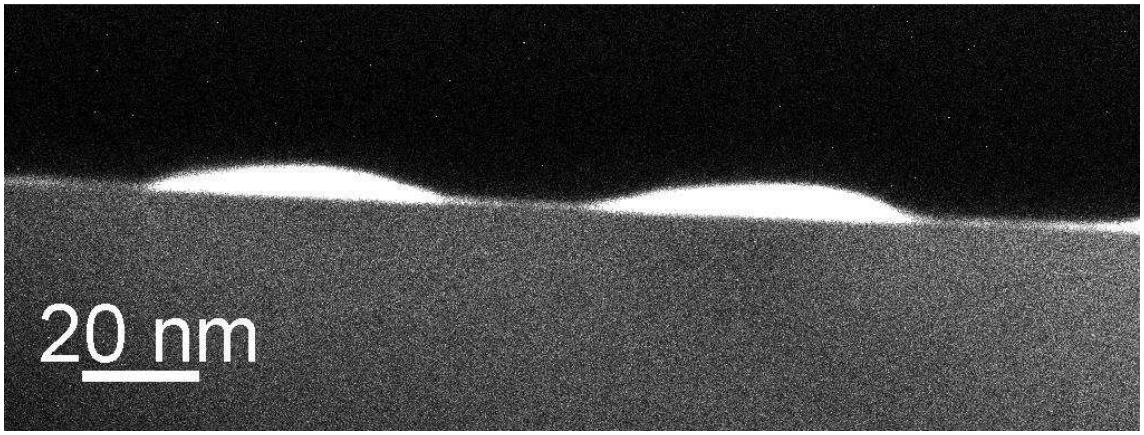

Figure 6. Annular Dark Field image of dilated islands of Ge grown on (1$\bar{1}$0)Si. Note ~20° sidewall inclination.

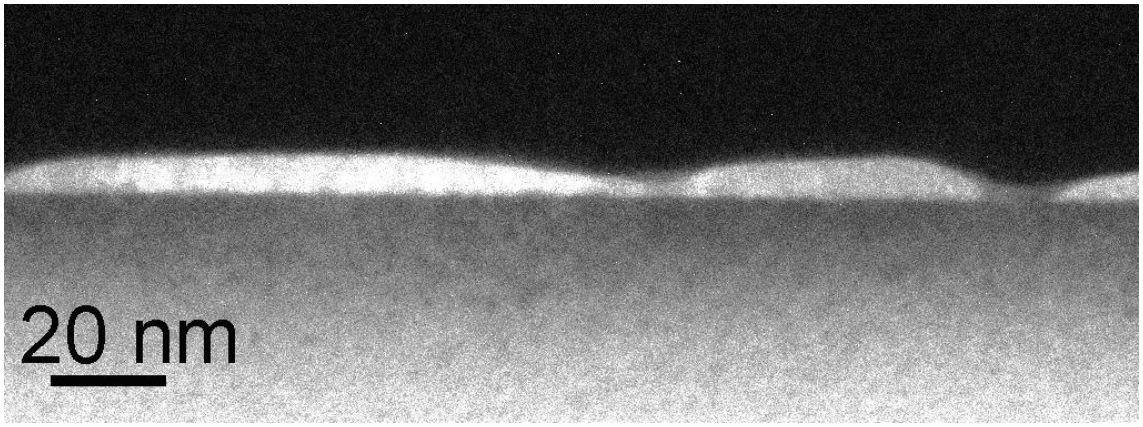

Figure 7. Annular Dark Field image of near continuous layer of Ge grown on (1$\bar{1}$1)Si

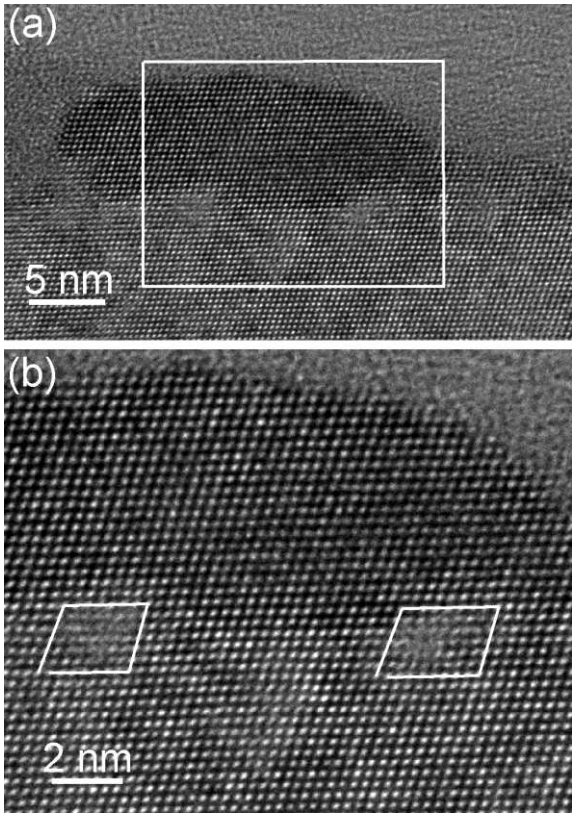

Figure 8. High Resolution phase contrast image of island showing amorphous-like regions at the boundary between the island and underlying (1$\bar{1}$1)Si wafer; (b) a magnified image of the interface with a Burgers' circuit drawn about the amorphous-like regions showing non-closure due to the cores of dislocations with Burgers vector component $\mathbf{b}_e$=¼ a [$\bar{1}$12].

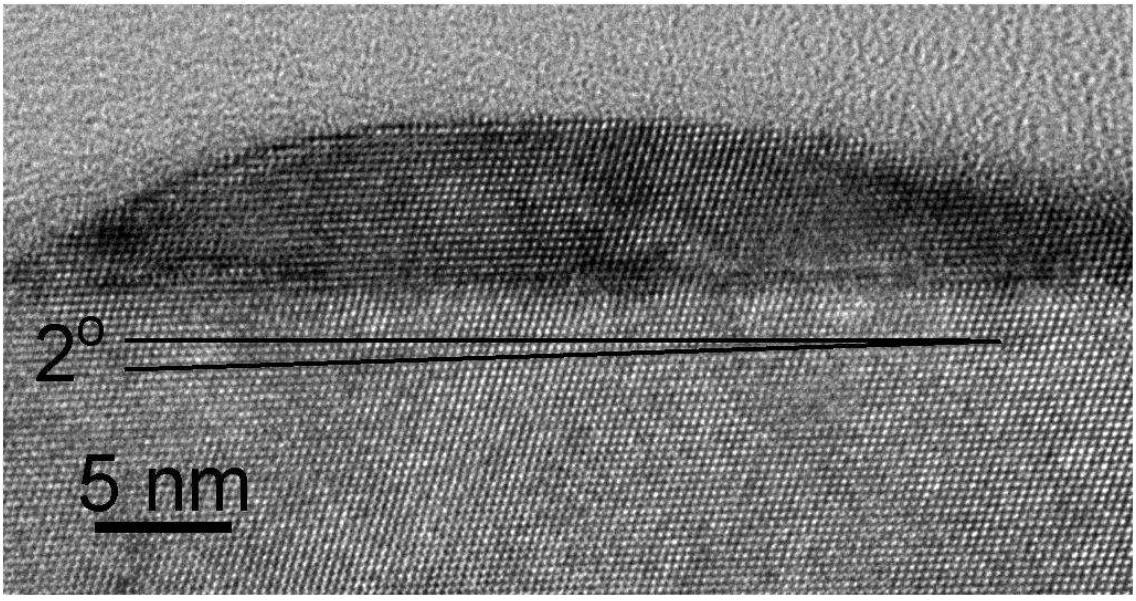

Figure 9. A phase contrast image showing the existence of a slight offcut between the Ge island and the underlying (1$\bar{1}$1)Si.

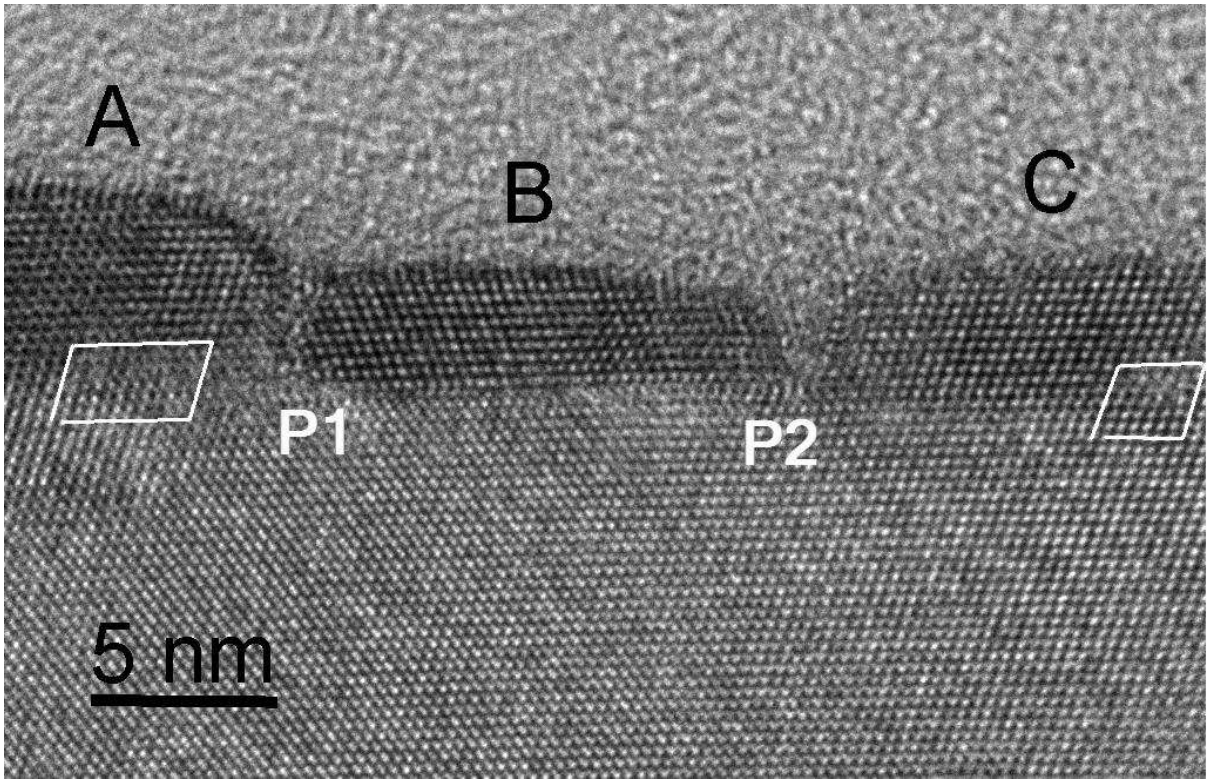

Figure 10. Phase contrast image showing the existence of twinned grains. Grain (B) is the twinned configuration of grains (A) and (C) and is bounded by partial dislocations P1 and P2. Grains A and C show the same dislocation structure as figure 8.

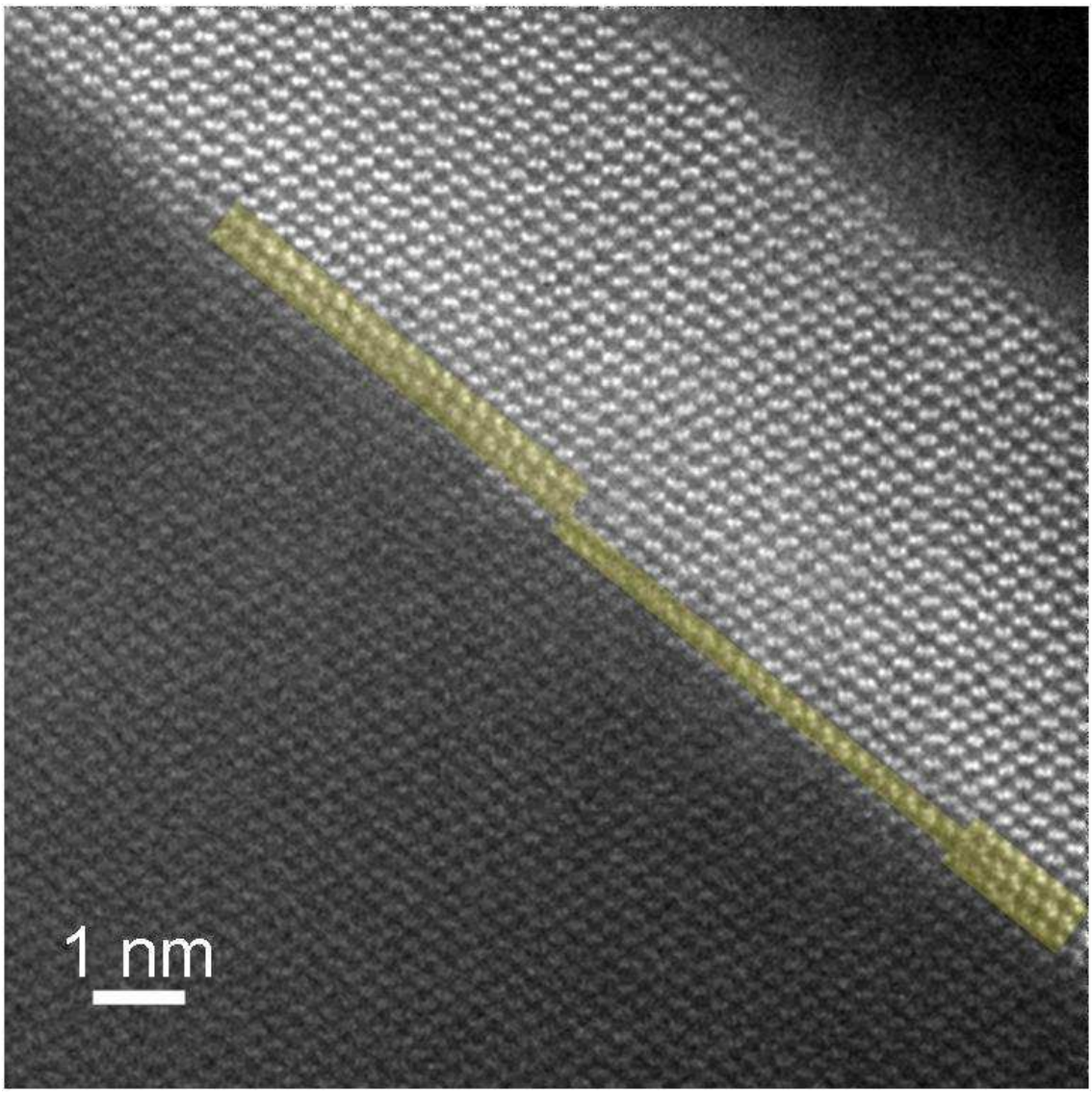

Figure 11. High Resolution Annular Dark-Field image showing the existence of a twinned configuration at the boundary between the Ge island and the underlying (1$\bar{1}$1)Si. The microtwin with dumb-bells pointing upwards is 1, 2 or 3 bilayers (=half unit cells) thick and has been marked in yellow. (reproduced from Norris et al. 2011)